

Stress Analysis of Asymmetrical Cold Rolling of Clad Sheet Using the Slab Method

Y.M. Hwang and G.Y. Tzou

An analytical model for general asymmetrical cold rolling of clad sheet bonded before rolling was proposed to explore the plastic deformation behavior of the clad sheet using the slab method. The model allowed easy calculation of the neutral points between the upper and lower rolls and the clad sheet; rolling pressure distribution along the contact interface of the roll, horizontal stresses in the component layers of the clad sheet, shear stresses at the interface of the clad sheet, and rolling force. These characteristics as affected by various rolling conditions (e.g., thickness ratio and shear yield stress ratio of the raw clad sheet, roll speed ratio, reduction, frictional coefficient, roll radius ratio, etc.) were analyzed systematically. This approach yielded complete forms for the rolling pressure distribution, rolling force, and rolling torque. Moreover, the computational time required by this analytical model is about 1/20 to 1/25 of that required by the RUNGE KUTTA numerical method under the same rolling conditions.

Keywords
asymmetrical cold rolling, clad sheet

1. Introduction

CLAD SHEETS with good anticorrosion, antirattling, or antifriction properties are now widely used in various industries. The production of clad sheets by rolling, which is more efficient and economical compared to other types of processes, has become an increasingly important subject of study. Due to the difference between the flow stresses of sheets, clad sheet rolling essentially belongs to the category of asymmetrical sheet rolling. Studies of clad sheet rolling rely largely on experimental approaches (Ref 1-6). Analyses using the upper-bound theorem have been proposed by one of the present authors (Ref 7-10) to investigate the characteristics of asymmetrical rolling of clad metal. The major disadvantage of the upper-bound theorem is that the rolling pressure distribution cannot be obtained. Suzuki et al. (Ref 11, 12) used the slab method and the RUNGE KUTTA numerical method to analyze the stress distribution at the roll gap during cold rolling of clad sheet. However, a lengthy computer calculation time is required by the numerical method, and rolling conditions are limited to identical radii or speeds of the upper and lower rolls.

An analytical model for asymmetrical cold strip rolling has been developed by the present authors (Ref 13). In this paper, the approach proposed earlier will be extended to simulate the plastic deformation mechanism of the clad sheet at the roll gap. Rolling pressure distributions, rolling forces, rolling torques, stress distributions at the roll gap under different roll radii and speeds, and so forth, will be systematically discussed.

Y.M. Hwang and **G.Y. Tzou,** Department of Mechanical Engineering, National Sun Yat-Sen University, Kaohsiung, Taiwan 80424, Republic of China; Fax: 886-7-551-8853

2. Mathematical Model

Figure 1 schematically illustrates asymmetrical rolling of clad sheet bonded before rolling. The radius and speed of the upper roll are different from those of the lower roll. The plastic deformation region at the roll gap is divided into three distinct regions, as in the case of single sheet rolling (Ref 13). These regions are denoted as zone I for the entrance region, zone II for the cross-shear region, and zone III for the exit region. The sub-

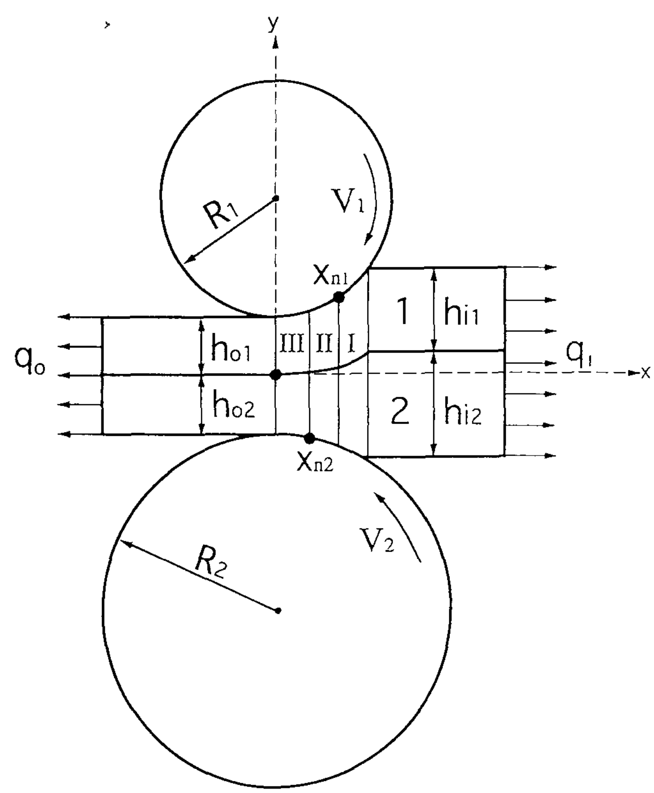

Fig. 1 Schematic illustration of asymmetrical rolling of clad sheet

scripts 1 and 2 in all variables represent the upper and lower rolls or layers, respectively.

2.1 *Assumptions*

To simplify the formulation involved in developing the analysis of stresses in cold clad sheet rolling based on the slab method, the following assumptions are made:

- The rolls are rigid; the sheets being rolled are rigid-plastic.
- The plastic deformation is plane strain.
- Stresses are uniformly distributed within elements. The vertical stress (p) and horizontal stresses (q_1 and q_2) are regarded as principal stresses.
- Frictional coefficients (μ_1 and μ_2) between the rolls and sheet are constant over the contact arc, but the frictional coefficient at the upper roll (μ_1) may be different from that at the lower roll (μ_2). The coulomb friction is assumed; that is, $\tau_1 = \mu_1 p_1$ and $\tau_2 = \mu_2 p_2$.
- The flow directions of sheets at the entrance and exit of the roll gap are horizontal.
- The total contact arc of the roll is much smaller than the circumference of the roll.
- There is no sliding between the interface of the clad sheet; that is, the clad sheet is bonded firmly before rolling.

2.2 *Formulation*

Figure 2 shows the element geometry at the roll gap. Figure 3 illustrates the stress state of the clad sheet in zone I, in which the directions of the upper and lower frictional forces are both forward; that is, the velocities of the upper and lower rolls are both greater than that of the clad sheet.

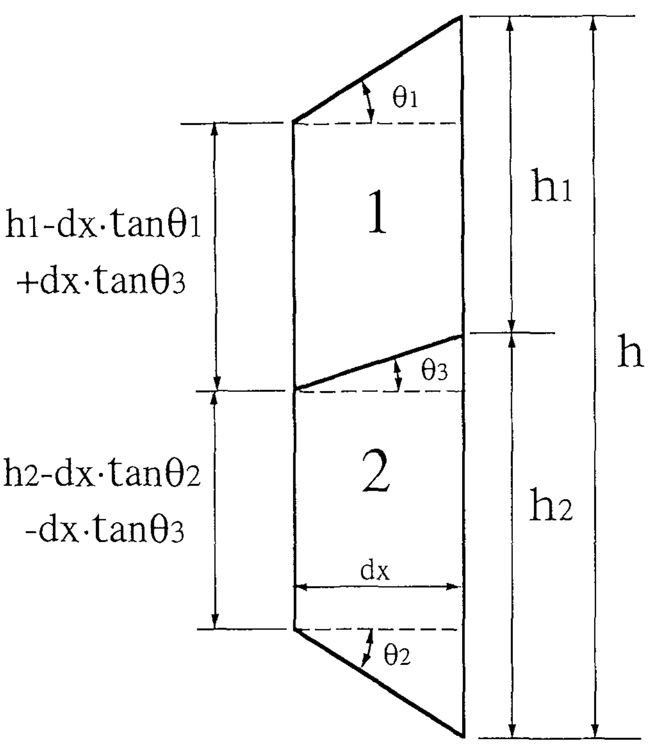

Fig. 2 Element geometry at the roll gap

The mathematical expressions for the horizontal and vertical force equilibriums in layer 1 (upper layer) and layer 2 (lower layer) can be summarized as:

$$\frac{d(h_1 q_1)}{dx} + p_1 \tan\theta_1 - p_3 \tan\theta_3 - \tau_1 + \tau_o = 0 \qquad \text{(Eq 1)}$$

$$p = p_1 + \tau_1 \tan\theta_1 = p_3 + \tau_o \tan\theta_3 \qquad \text{(Eq 2)}$$

and

$$\frac{d(h_2 q_2)}{dx} + p_2 \tan\theta_2 + p_3 \tan\theta_3 - \tau_2 - \tau_o = 0 \qquad \text{(Eq 3)}$$

$$p = p_2 + \tau_2 \tan\theta_2 = p_3 + \tau_o \tan\theta_3 \qquad \text{(Eq 4)}$$

where q, p, and h denote horizontal stress, vertical stress, and thickness, respectively; θ_1 and θ_2 are variable contact angles; τ_o is the shear stress at the interface of the clad sheet; $\tau_1 = \mu_1 p_1$ and $\tau_2 = \mu_2 p_2$ are frictional stresses along the upper and lower roll boundaries, respectively; p_1 and p_2 are rolling pressures of

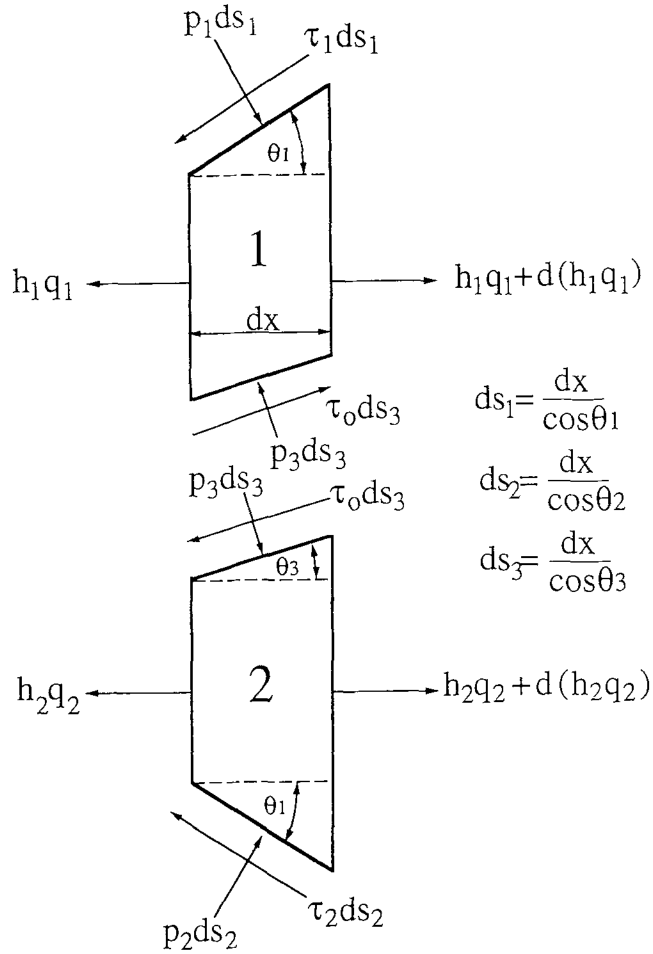

Fig. 3 Slab stress state of clad sheet in zone I

the upper and lower rolls; and p_3 is the contact pressure at the bonded interface.

Combining Eq 1 and 2 and Eq 3 and 4 gives:

$$\frac{d(h_1q_1)}{dx} + \Theta_1 p + \Theta_3\tau_o = 0 \quad \text{(Eq 5)}$$

$$\frac{d(h_2q_2)}{dx} + \Theta_2 p - \Theta_3\tau_o = 0 \quad \text{(Eq 6)}$$

where

$$\Theta_1 = \frac{\tan\theta_1 - \mu_1}{1 + \mu_1 \tan\theta_1} - \tan\theta_3$$

$$\Theta_2 = \frac{\tan\theta_2 - \mu_2}{1 + \mu_2 \tan\theta_2} + \tan\theta_3$$

$$\Theta_3 = 1 + \tan^2\theta_3$$

Combining Eq 5 and 6 then yields:

$$\frac{d(hq)}{dx} + (\Theta_1 + \Theta_2)p = 0 \quad \text{(Eq 7)}$$

where $hq = h_1q_1 + h_2q_2$. Equation 7 is the differential equation derived from the force equilibrium for a clad sheet at the roll gap.

The von Mises yield criterion for plane strain within layers 1 and 2 can be expressed, respectively, as:

$$p + q_1 = 2k_1 \quad \text{(Eq 8)}$$

and

$$p + q_2 = 2k_2 \quad \text{(Eq 9)}$$

where

$$k_1 = \frac{\sigma_{yp1}}{\sqrt{3}},$$

$$k_2 = \frac{\sigma_{yp2}}{\sqrt{3}}$$

The terms σ_{yp1} and σ_{yp2} are the mean uniaxial yield stresses of the upper and lower layers, respectively. Complying with $hq = h_1q_1 + h_2q_2$, the yield criterion for the clad sheet can be derived as:

$$p + q = 2k_1\beta + 2k_2(1 - \beta) \quad \text{(Eq 10)}$$

where

$$\beta = \frac{h_1}{h} = \frac{h_{i1}}{h_i} = \frac{h_{o1}}{h_o}$$

where β is the thickness ratio of the upper layer to the clad sheet, and h_o and h_i are the thicknesses of the clad sheet at the exit and entrance at the roll gap, respectively. From Fig. 2, some geometry relationships at the roll gap can be obtained:

$$h = h_1 + h_2 = h_o + \frac{x^2}{R_{eq}}, \frac{dh}{dx} = \frac{2x}{R_{eq}}, \tan\theta_1 = \frac{x}{R_1}, \tan\theta_2 = \frac{x}{R_2} \quad \text{(Eq 11)}$$

where R_{eq} is the effective roll radius:

$$R_{eq} = \frac{2R_1R_2}{R_1 + R_2}$$

The relationships among θ_3, θ_2, and θ_1 can be obtained from the conception of the same thickness ratio at the roll gap as:

$$\tan\theta_3 = (1 - \beta)\tan\theta_1 - \beta\tan\theta_2 \quad \text{(Eq 12)}$$

Because the roll radius is much larger than the thickness of the clad sheet, $1 + \mu_1 \tan\theta_1$ and $1 + \mu_2 \tan\theta_2$ in Eq 7 are approximately eqùal to 1, which indicates $p \doteq p_1 \doteq p_2$. Thus, combining the previous geometry relations, Eq 7 becomes:

$$h\frac{dq}{dx} + (p + q)\frac{dh}{dx} = \mu_e p \quad \text{(Eq 13)}$$

where $\mu_e = \mu_1 + \mu_2$ is the equivalent frictional coefficient.

Substituting Eq 10 into Eq 13 and rearranging it produces:

$$(1 + z^2)\frac{df}{dz} + af = 2\alpha z \quad \text{(Eq 14)}$$

where

$$a = \mu_e\sqrt{\frac{R_{eq}}{h_o}}, \alpha = \beta + \frac{k_2}{k_1}(1 - \beta), z = \frac{x}{\sqrt{R_{eq}h_o}}, f = \frac{p}{2k_1}$$

Introducing parameter ω as:

$$z = \tan\omega \quad \text{(Eq 15)}$$

Equation 14 becomes:

$$\frac{df}{d\omega} + af = 2\alpha\tan\omega \quad \text{(Eq 16)}$$

Conventionally, when ω is small, $\tan\omega$ in Eq 15 can be approximately expressed as:

$$\tan\omega \doteqdot \omega \quad \text{(Eq 17)}$$

However, more precisely, one adopts:

$$\tan\omega \doteqdot \omega + \frac{\omega^3}{3} \quad \text{(Eq 18)}$$

The solution of Eq 16 is:

$$f = ce^{-a\omega} + \frac{2\alpha}{a}\left(\frac{\omega^3}{3} - \frac{\omega^2}{a} + s\omega - t\right) \quad \text{(Eq 19)}$$

where

$$s = 1 + \frac{2}{a^2},\ t = \frac{1}{a} + \frac{2}{a^3}$$

where c in Eq 19 is the integral constant determined by the boundary condition. Equation 19, valid for zones I, II, and III, is a general form for specific rolling pressure. The shear stress (τ_o) at the interface of the clad sheet can be obtained by combining Eq 5 and 6 as:

$$\tau_o = \frac{\Theta_1 \dfrac{d(h_2q_2)}{dx} - \Theta_2 \dfrac{d(h_1q_1)}{dx}}{\Theta_3(\Theta_1 + \Theta_2)} \quad \text{(Eq 20)}$$

In zone III, because the directions of frictional force are backward (i.e., the strip velocity is greater than that of the upper and lower rolls), the form of the differential equation in zone III is the same as that in zone I, except that the equivalent frictional coefficient μ_e is replaced by $\mu_e = -\mu_1 - \mu_2$. In zone II, because the directions of frictional force are opposite to each other (i.e., the strip velocity is greater than that of the upper roll and less than that of the lower roll, if $V_2 > V_1$ is assumed), then $\mu_e = -\mu_1 + \mu_2$.

2.3 *Boundary Conditions*

Assuming that the velocity of the lower roll is greater than that of the upper roll, and that the neutral point of the upper roll is denoted by x_{n1} and the neutral point of the lower roll by x_{n2}, the boundary conditions for the three distinct regions can be expressed as shown in the following sections.

2.3.1 Zone III ($0 \le x \le x_{n2}$), $\mu_e = -\mu_1 - \mu_2$

At x = 0 (or ω = 0):

$$f_o = \alpha - \frac{q_o}{2k_1}$$

where q_o is the front tension exerted on the clad sheet. From this boundary condition, integral constant c_3 in Eq 19 can be obtained as:

$$c_3 = f_o + \frac{2\alpha t_3}{a_3} \quad \text{(Eq 21)}$$

where

$$t_3 = \frac{1}{a_3} + \frac{2}{a_3^3},\ s_3 = 1 + \frac{2}{a_3^2}$$

Hence, the specific rolling pressure (f_{III}) in zone III is expressed as:

$$f_{III} = c_3 e^{-a_3\omega} + \frac{2\alpha}{a_3}\left(\frac{\omega^3}{3} - \frac{\omega^2}{a_3} + s_3\omega - t_3\right) \quad \text{(Eq 22)}$$

The specific shear stress (τ_o/k_1) in zone III can be obtained as:

$$\left(\frac{\tau_o}{k_1}\right)_{III} = \frac{\Theta_1\Theta_{43} - \Theta_2\Theta_{53}}{\Theta_6} \quad \text{(Eq 23)}$$

where

$$\Theta_1 = \frac{2\beta x}{R_{eq}} + \mu_1,\ \Theta_2 = \frac{2(1-\beta)x}{R_{eq}} + \mu_2,$$

$$\Theta_6 = \frac{2D}{R_{eq}}x^3 - D\mu_e x^2 + \frac{2x}{R_{eq}} - \mu_e$$

$$\Theta_{43} = \frac{2(1-\beta)\sqrt{R_{eq}h_o}}{R_{eq}}\left[c_3a_3e^{-a_3\omega} - \frac{2\alpha}{a_3}\left(\omega^2 - \frac{2\omega}{a_3} + s_3\right)\right] + (2k_2 - p_{III})\frac{2(1-\beta)x}{R_{eq}k_1}$$

$$\Theta_{53} = \frac{2\beta\sqrt{R_{eq}h_o}}{R_{eq}}\left[c_3a_3e^{-a_3\omega} - \frac{2\alpha}{a_3}\left(\omega^2 - \frac{2\omega}{a_3} + s_3\right)\right] + (2k_1 - p_{III})\frac{2\beta x}{R_{eq}k_1}$$

$$D = \left(\frac{1}{R_1} - \frac{2\beta}{R_{eq}}\right)^2$$

2.3.2 Zone I ($x_{n1} \le x \le L$), $\mu_e = \mu_1 + \mu_2$

At $x = L$ (or $\omega = \omega_i = \tan^{-1}L/\sqrt{R_{eq}h_o}$):

$$f_i = \alpha - \frac{q_i}{2k_1}$$

where q_i is the back tension exerted on the clad sheet, and L is the contact length at the roll gap. From this boundary condition, c_1 in Eq 19 is expressed as:

$$c_1 = \left[f_i - \frac{2\alpha}{a_1}\left(\frac{\omega_i^3}{3} - \frac{\omega_i^2}{a_1} + s_1\,\omega_i - t_1\right)\right] e^{a_1\omega_i} \quad \text{(Eq 24)}$$

Therefore, the specific rolling pressure (f_I) in zone I can be expressed as:

$$f_I = c_1 e^{-a_1\omega} + \frac{2\alpha}{a_1}\left(\frac{\omega^3}{3} - \frac{\omega^2}{a_1} + s_1\,\omega - t_1\right) \quad \text{(Eq 25)}$$

where

$$t_1 = \frac{1}{a_1} + \frac{2}{a_1^3},\ s_1 = 1 + \frac{2}{a_1^2}$$

The specific shear stress (τ_o/k_1) in zone I can be obtained as:

$$\left(\frac{\tau_o}{k_1}\right)_I = \frac{\Theta_1\,\Theta_{41} - \Theta_2\,\Theta_{51}}{\Theta_6} \quad \text{(Eq 26)}$$

where

$$\Theta_1 = \frac{2\beta x}{R_{eq}} - \mu_1,\ \Theta_2 = \frac{2(1-\beta)x}{R_{eq}} - \mu_2$$

$$\Theta_{41} = \frac{2(1-\beta)\sqrt{R_{eq}h_o}}{R_{eq}}\left[c_1 a_1 e^{-a_1\omega} - \frac{2\alpha}{a_1}\left(\omega^2 - \frac{2\omega}{a_1} + s_1\right)\right] + (2k_2 - p_I)\frac{2(1-\beta)x}{R_{eq}k_1}$$

$$\Theta_{51} = \frac{2\beta\sqrt{R_{eq}h_o}}{R_{eq}}\left[c_1 a_1 e^{-a_1\omega} - \frac{2\alpha}{a_1}\left(\omega^2 - \frac{2\omega}{a_1} + s_1\right)\right] + (2k_1 - p_I)\frac{2\beta x}{R_{eq}k_1}$$

When the peripheral velocity of the upper roll (V_1) is less than that of the lower roll (V_2), the region of x for zone II is $x_{n2} \le x \le x_{n1}$ and $\mu_e = -\mu_1 + \mu_2$.

2.3.3 Zone II ($x_{n2} \le x \le x_{n1}$), $\mu_3 = -\mu_1 + \mu_2$

The specific rolling pressure (f_{II}) in zone II is expressed as:

$$f_{II} = c_2 e^{-a_2\omega} + \frac{2\alpha}{a_2}\left(\frac{\omega^3}{3} - \frac{\omega^2}{a_2} + s_2\omega - t_2\right) \quad \text{(Eq 27)}$$

where

$$t_2 = \frac{1}{a_2} + \frac{2}{a_2^3},\ s_2 = 1 + \frac{2}{a_2^2}$$

Due to the continuity of boundary conditions at $x = x_{n2}$ (or $\omega = \omega_{n2}$), the specific rolling pressure in zone III (f_{III}) at $x = x_{n2}$ must be identical to that in zone II (f_{II}), that is, $f_{III} = f_{II}$. Therefore, c_3 and c_2 have the following relationship:

$$c_2 = c_3 e^{B_1\omega_{n2}} + \alpha e^{a_2\omega_{n2}}\left(B_2\omega_{n2}^3 - B_3\omega_{n2}^2 + B_4\omega_{n2} - B_5\right) \quad \text{(Eq 28)}$$

where

$$B_1 = a_2 - a_3,\ B_2 = \frac{2}{3a_3} - \frac{2}{3a_2},\ B_3 = \frac{2}{a_3^2} - \frac{2}{a_2^2}$$

$$B_4 = \frac{2s_3}{a_3} - \frac{2s_2}{a_2},\ B_5 = \frac{2t_3}{a_3} - \frac{2t_2}{a_2},\ \omega_{n2} = \tan^{-1}\frac{x_{n2}}{\sqrt{R_{eq}h_o}}$$

Similarly, in light of the continuity of boundary conditions at $x = x_{n1}$, (i.e., $f_I = f_{II}$), c_1 and c_2 have the following relationship:

$$c_2 = c_1\,e^{B_6\omega_{n1}} + \alpha\,e^{a_2\omega_{n1}}\left(B_7\,\omega_{n1}^3 - B_8\,\omega_{n1}^2 + B_9\omega_{n1} - B_{10}\right) \quad \text{(Eq 29)}$$

where

$$B_6 = a_2 - a_1,\ B_7 = \frac{2}{3a_1} - \frac{2}{3a_2},\ B_8 = \frac{2}{a_1^2} - \frac{2}{a_2^2}$$

$$B_9 = \frac{2s_1}{a_1} - \frac{2s_2}{a_2},\ B_{10} = \frac{2t_1}{a_1} - \frac{2t_2}{a_2},\ \omega_{n1} = \tan^{-1}\frac{x_{n1}}{\sqrt{R_{eq}h_o}}$$

Combining Eq 28 and 29 provides:

$$c_3 e^{B_1\omega_{n2}} + \alpha e^{a_2\omega_{n2}}\left(B_2\,\omega_{n2}^3 - B_3\omega_{n2}^2 + B_4\,\omega_{n2} - B_5\right) = c_1 e^{B_6\omega_{n1}} + \alpha e^{a_2\omega_{n1}}\left(B_7\omega_{n1}^3 - B_8\omega_{n1}^2 + B_9\omega_{n1} - B_{10}\right) \quad \text{(Eq 30)}$$

From the constancy of volume, the positions of the upper and lower neutral points x_{n1} and x_{n2} have the following relationship:

$$x_{n1} = \sqrt{V_A x_{n2}^2 + (V_A - 1)\frac{h_o}{R_A}} \quad \text{(Eq 31)}$$

where

$$V_A = \frac{V_2}{V_1}, R_A = \frac{1}{R_{eq}} - \frac{h_o}{2R_{eq}^2}$$

Substituting Eq 31 into Eq 30, the solution of the neutral point x_{n2} can easily be found using the bisection numerical method. Once x_{n2} is known, x_{n1} and c_2 can be obtained from Eq 31 and 28. The specific shear stress (τ_o/k_1) in zone II can be obtained as:

$$\left(\frac{\tau_o}{k_1}\right)_{II} = \frac{\Theta_1 \Theta_{42} - \Theta_2 \Theta_{52}}{\Theta_6} \quad \text{(Eq 32)}$$

where

$$\Theta_1 = \frac{2\beta x}{R_{eq}} + \mu_1, \Theta_2 = \frac{2(1-\beta)x}{R_{eq}} - \mu_2$$

$$\Theta_{42} = \frac{2(1-\beta)\sqrt{R_{eq}h_o}}{R_{eq}}\left[c_2 a_2 e^{-a_2\omega} - \frac{2\alpha}{a_2}\left(\omega^2 - \frac{2\omega}{a_2} + s_2\right)\right] + (2k_2 - p_{II})\frac{2(1-\beta)x}{R_{eq}k_1}$$

$$\Theta_{52} = \frac{2\beta\sqrt{R_{eq}h_o}}{R_{eq}}\left[c_2 a_2 e^{-a_2\omega} - \frac{2\alpha}{a_2}\left(\omega^2 - \frac{2\omega}{a_2} + s_2\right)\right] + (2k_1 - p_{II})\frac{2\beta x}{R_{eq}k_1}$$

2.4 *Rolling Force*

Once the mean shear yield stresses and frictional coefficients are known, the rolling force can be found by integrating the normal rolling pressure over the arc length of contact. Thus, the rolling force per unit width, P, is given by:

$$P = P_{III} + P_{II} + P_I \quad \text{(Eq 33)}$$

where

$$P_{III} = 2k_1 \int_0^{x_{n2}} f_{III}\, dx = 2k_1 \sqrt{R_{eq}h_o}\,(III_1 + III_2) \quad \text{(Eq 34)}$$

$$III_1 = \frac{-c_3 e^{a_3\omega_{n2}}}{a_3}\left(1 + \omega_{n2}^2 + 2\frac{\omega_{n2}}{a_3} + \frac{2}{a_3^2}\right) + \frac{c_3}{a_3} + 2\frac{c_3}{a_3^3}$$

$$III_2 = \alpha\left[\frac{\omega_{n2}^6}{9a_3} - \frac{2\omega_{n2}^5}{5a_3^2} + \frac{1/3 + s_3}{2a_3}\omega_{n2}^4 - \frac{2}{3a_3}\left(\frac{1}{a_3} + t_3\right)\omega_{n2}^3 + \frac{s_3\,\omega_{n2}^2}{a_3} - \frac{2t_3\,\omega_{n2}}{a_3}\right]$$

$$P_{II} = 2k_1 \int_{x_{n2}}^{x_{n1}} f_{II}\, dx = 2k_1 \sqrt{R_{eq}h_o}\,(II_1 + II_2) \quad \text{(Eq 35)}$$

$$II_1 = \frac{-c_2 e^{-a_2\omega_{n1}}}{a_2}\left(1 + \omega_{n1}^2 + \frac{2\omega_{n1}}{a_2} + \frac{2}{a_2^2}\right) + \alpha\left[\frac{\omega_{n1}^6}{9a_2} - \frac{2\omega_{n1}^5}{5a_2^2} + \frac{1/3 + s_2}{2a_2}\omega_{n1}^4 - \frac{2}{3a_2}\left(\frac{1}{a_2} + t_2\right)\omega_{n1}^3 + \frac{s_2}{a_2}\omega_{n1}^2 - \frac{2t_2}{a_2}\omega_{n1}\right]$$

$$II_2 = \frac{c_2 e^{-a_2\omega_{n2}}}{a_2}\left(1 + \omega_{n2}^2 + \frac{2\omega_{n2}}{a_2} + \frac{2}{a_2^2}\right) - \alpha\left[\frac{\omega_{n2}^6}{9a_2} - \frac{2\omega_{n2}^5}{5a_2^2} + \frac{1/3 + s_2}{2a_2}\omega_{n2}^4 - \frac{2}{3a_2}\left(\frac{1}{a_2} + t_2\right)\omega_{n2}^3 + \frac{s_2}{a_2}\omega_{n2}^2 - \frac{2t_2}{a_2}\omega_{n2}\right]$$

$$P_I = 2k_1 \int_{x_{n1}}^{L} f_I\, dx = 2k_1 \sqrt{R_{eq}h_o}\,(I_1 + I_2) \quad \text{(Eq 36)}$$

$$I_1 = \frac{-c_1 e^{-a_1\omega_i}}{a_1}\left(1 + \omega_i^2 + \frac{2\omega_i}{a_1} + \frac{2}{a_1^2}\right) + \alpha\left[\frac{\omega_i^6}{9a_1} - \frac{2\omega_i^5}{5a_1^2} + \frac{1/3 + s_1}{2a_1}\omega_i^4 - \frac{2}{3a_1}\left(\frac{1}{a_1} + t_1\right)\omega_i^3 + \frac{s_1\omega_i^2}{a_1} - \frac{2t_1\omega_i}{a_1}\right]$$

$$I_2 = \frac{c_1 e^{-a_1\omega_{n1}}}{a_1}\left(1 + \omega_{n1}^2 + \frac{2\omega_{n1}}{a_1} + \frac{2}{a_1^2}\right) - \alpha\left[\frac{\omega_{n1}^6}{9a_1} - \frac{2\omega_{n1}^5}{5a_1^2} + \frac{1/3 + s_1}{2a_1}\omega_{n1}^4 - \frac{2}{3a_1}\left(\frac{1}{a_1} + t_1\right)\omega_{n1}^3 + \frac{s_1\omega_{n1}^2}{a_1} - \frac{2t_1\omega_{n1}}{a_1}\right]$$

2.5. *Rolling Torque*

The rolling torques, T_1 and T_2, exerted by the clad sheet on the upper and lower rolls, respectively, can be calculated by integrating the moment of the frictional force along the arc of contact about the roll axis. Therefore:

$$T_1 = R_1(\mu_1 P_I - \mu_1 P_{II} - \mu_1 P_{III}) = \mu_1 R_1(P_I - P_{II} - P_{III}) \quad \text{(Eq 37)}$$

$$T_2 = R_2(\mu_2 P_I + \mu_2 P_{II} - \mu_2 P_{III}) = \mu_2 R_2(P_I + P_{II} - P_{III}) \quad \text{(Eq 38)}$$

and the total rolling torque required, T, is

$$T = T_1 + T_2 \quad \text{(Eq 39)}$$

2.6 *Special Case*

When the frictional coefficient between the upper roll and layer 1 (μ_1) equals that between the lower roll and layer 2 (μ_2), the formulations given for zone II are no longer applied, because μ_e (or a_2) is zero in zone II. Thus, the equations derived previously for pressure distributions become meaningless, and modifications must be made.

From Eq 13, if μ_e is zero, the specific rolling pressure in zone II can be expressed as:

$$f_{II} = \alpha \ln h + c_2 \quad \text{(Eq 40)}$$

where c_2 is the integral constant determined by boundary conditions. Following the same procedures with the same boundary conditions as described earlier, the equation used to find the neutral point x_{n2} can be expressed as:

$$c_1 e^{-a_1\omega_{n1}} + \frac{2\alpha}{a_1}\left(\frac{\omega_{n1}^3}{3} - \frac{\omega_{n1}^2}{a_1} + s_1\,\omega_{n1}\right) - c_3 e^{-a_3\omega_{n2}} - \frac{2\alpha}{a_3}\left(\frac{\omega_{n2}^3}{3} - \frac{\omega_{n2}^2}{a_3} + s_3\,\omega_{n2}\right) - F = 0 \quad \text{(Eq 41)}$$

where

$$F = \alpha\left(\ln\frac{h_{n1}}{h_{n2}} + \frac{2t_1}{a_1} - \frac{2t_3}{a_3}\right)$$

Combining Eq 31 and 41, the neutral points x_{n2} and x_{n1} can be obtained, and c_2 is expressed as:

$$c_2 = c_3 e^{-a_3\omega_{n2}} + \frac{2\alpha}{a_3}\left(\frac{\omega_{n2}^3}{3} - \frac{\omega_{n2}^2}{a_3} + s_3\,\omega_{n2} - t_3\right) - \alpha \ln h_{n2} \quad \text{(Eq 42)}$$

The rolling force per unit width in zone II can be derived as:

$$P_{II} = 2k_1 \int_{x_{n2}}^{x_{n1}} f_{II}\,dx = 2k_1[\alpha \mathrm{II}_n + c_2(x_{n1} - x_{n2})] \quad \text{(Eq 43)}$$

where

$$\mathrm{II}_n = x_{n1}\ln h_{n1} - 2x_{n1} + 2\sqrt{R_{eq}\,h_o}\,\omega_{n1} - x_{n2}\ln h_{n2} + 2x_{n2} - 2\sqrt{R_{eq}\,h_o}\,\omega_2$$

$$h_{n2} = h_o + \frac{x_{n2}^2}{R_{eq}},\ h_{n1} = h_o + \frac{x_{n1}^2}{R_{eq}}$$

The specific shear stress (τ_o/k_1) in zone II can be obtained as:

$$\left(\frac{\tau_o}{k_1}\right)_{II} = \frac{\Theta_1\,\Theta_{42}^* - \Theta_2\,\Theta_{52}^*}{\Theta_6} \quad \text{(Eq 44)}$$

where

$$\Theta_{42}^* = \frac{-4\alpha(1-\beta)x}{R_{eq}} + (2k_2 - p_{II})\frac{2(1-\beta)x}{R_{eq}k_1}$$

$$\Theta_{52}^* = \frac{-4\alpha\beta x}{R_{eq}} + (2k_1 - p_{II})\frac{2\beta x}{R_{eq}k_1}$$

It should be noted that Eq 40 to 44 are valid only for the case of $\mu_1 = \mu_2$.

3. Results and Discussion

The rolling conditions employed for the following numerical simulation under the conditions of different roll radii and speeds are summarized in Table 1. The main results will be discussed here.

Figure 4 shows various stress distributions at the roll gap under the conditions of different roll radii and speeds in an asymmetrical rolling of clad sheet. The upper layer is assumed to be softer than the lower layer. The specific rolling pressure, $p/2k_1$, and the specific horizontal stress for the whole clad sheet, $q/2k_1$, are compressive at the roll gap. It is noteworthy that the specific horizontal stress in the softer layer 1, $q_1/2k_1$, is compressive, whereas that in the harder layer 2, $q_2/2k_2$, is tensile or partially compressive. Because the frictional stresses along the upper and lower roll surfaces have the opposite direction in

Table 1 Conditions for asymmetrical cold rolling of clad sheet

Condition	V_2/V_1	R_2/R_1	k_2/k_1	β	$\mu_2 = \mu_1 = \mu$	r, %
1	1.1	1.1	2	~0.2-0.8	0.1	30
2	1.1	1.1	~1-4	0.2	0.1	30
3	1.1	1.1	2	0.8	0.1	~20-40
4	1.1	1.1	2	0.2	~0.1-0.2	30
5	1.1	~0.5-1.5	2	0.2	0.1	30
6	~1.05-1.2	1.1	2	0.2	0.2	30

Note: $R_1 = 100$ mm; $V_1 = 50$ mm/s; $k_1 = 98.1$ MPa; $q_1 = q_o = 0$; $h_i = 2$ mm

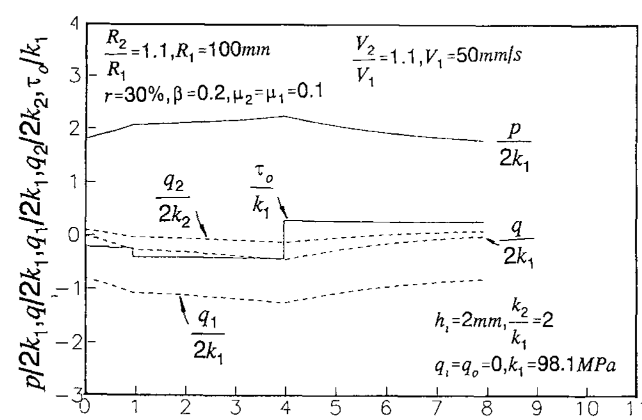

Fig. 4 Various stress distributions at the roll gap

zone II, the specific shear stress at the interface of layers in zone II, τ_0/k_1, has a higher value in zone II (cross-shear region), and the sign of τ_0 is opposite to that in zone I in light of the change in direction of the frictional force.

Figure 5 illustrates various stress distributions with different thickness ratios β under different roll radii and speeds. It can be seen that $p/2k_1$ and $q/2k_1$ decrease with increasing β, because the fraction of the soft layer 1 increases with the increase of β. It should be noted that $q_2/2k_2$ becomes tensile partially as β increases. The tensile stresses are not preferable, because they sometimes result in instability of the lower layer. The value of τ_0/k_1 decreases with the increase of β, but the sign of τ_0/k_1 is changed from zone I to zone II or from zone II to zone III as β is smaller than 0.5. Moreover, the magnitude of τ_0/k_1 is smaller than 1 which implies that good bonding should prevent sliding at the interface of the clad sheet. In the case of β = 0.5, where the thicknesses of the soft and hard layers are identical to each other, τ_0/k_1 in the exit region (zone III) is almost zero and very small in the entrance region. However, it is relatively large in the cross-shear region due to the opposite directions of frictional stresses along the upper and lower roll surfaces.

Effects of the shear yield stress ratio, k_2/k_1, on the various stress distributions at the roll gap are shown in Fig. 6, which in-

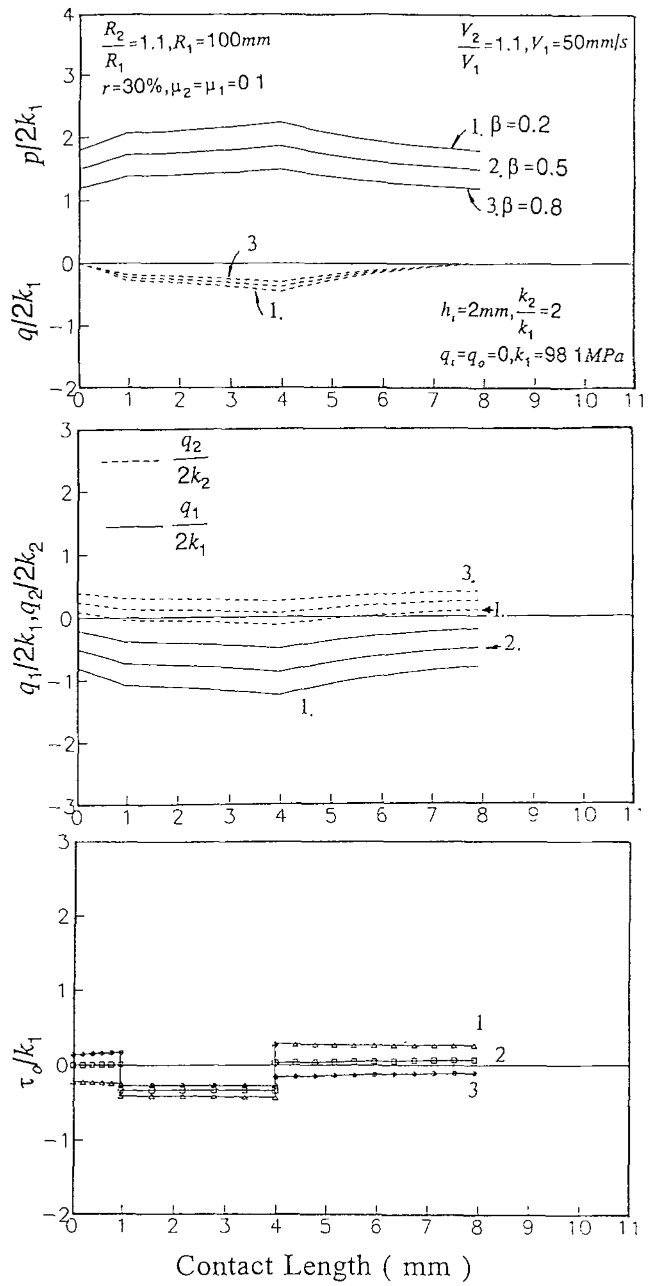

Fig. 5 Effects of thickness ratio, β, on various stress distributions at the roll gap

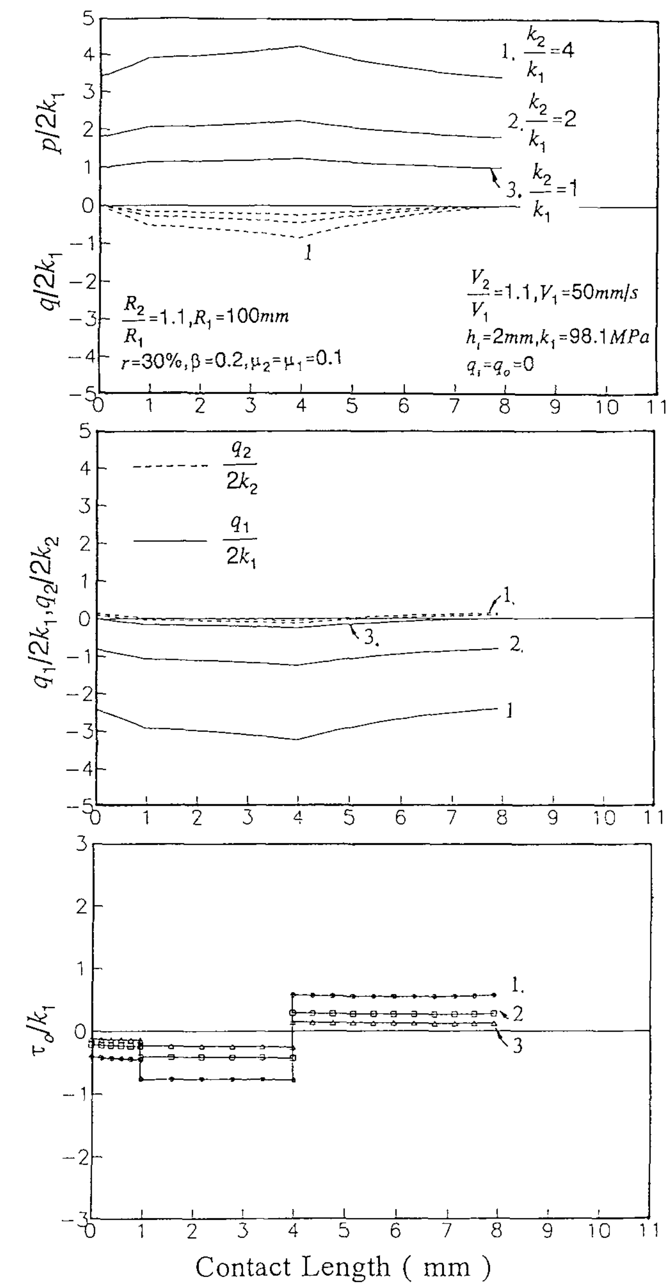

Fig. 6 Effects of yield stress ratio, k_2/k_1, on various stress distributions at the roll gap

dicates that $p/2k_1$ and $q/2k_1$ increase with increasing k_2/k_1 (as k_1 is fixed). That is because the shear yield stress of the hard layer 2 is larger as k_2/k_1 increases. It is also noted that $q_1/2k_1$ has larger compressive stresses, whereas $q_2/2k_2$ becomes tensile near the exit and entrance regions and changes slightly with the increase of k_2/k_1. Besides, τ_o/k_1 in zone II increases with the increase of k_2/k_1. If τ_o/k_1 is large enough (e.g., $\tau_o/k_1 > 1$), sliding at the interface of the clad sheet may take place.

Effects of the reduction, r, on the various stress distributions at the roll gap are demonstrated in Fig. 7. Obviously, $p/2k_1$ and $q/2k_1$ increase with an increase in reduction; $q_2/2k_2$ is tensile throughout the contact length, and the magnitude of $q_2/2k_2$ increases as reduction decreases. When reduction increases, τ_o/k_1 in the exit and entrance regions change slightly.

Figure 8 shows the effects of the frictional coefficient, μ, on the various stress distributions at the roll gap. As μ increases, the magnitude of $p/2k_1$, $q/2k_1$, and $q_1/2k_1$ increases, and $q_2/2k_2$ has larger compressive stress. On the contrary, when μ is smaller (e.g., $\mu = 0.1$), $q_2/2k_2$ is partially tensile. The magnitude of τ_o/k_1 increases and the cross-shear region becomes narrow as μ increases. It is noteworthy that in the case of $\mu = 0.2$, τ_o/k_1 in the cross-shear region exceeds 1, which means that the bonding may be destroyed and that sliding at the interface of the clad sheet may occur.

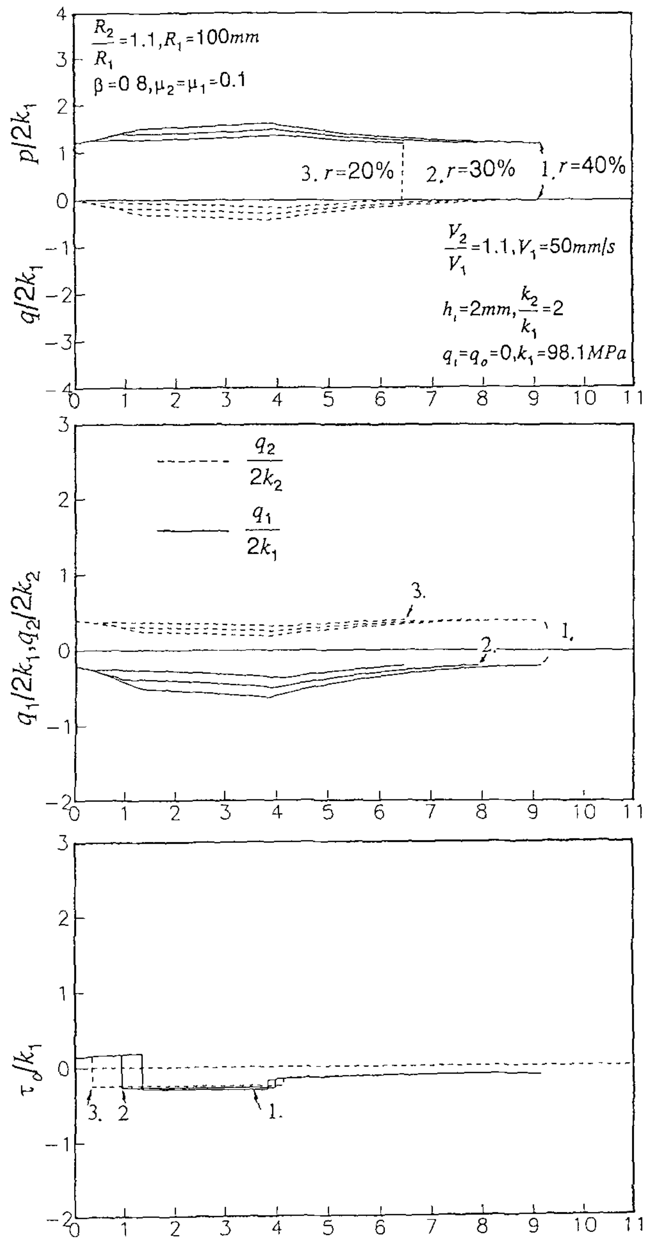

Fig. 7 Effects of reduction, r, on various stress distributions at the roll gap

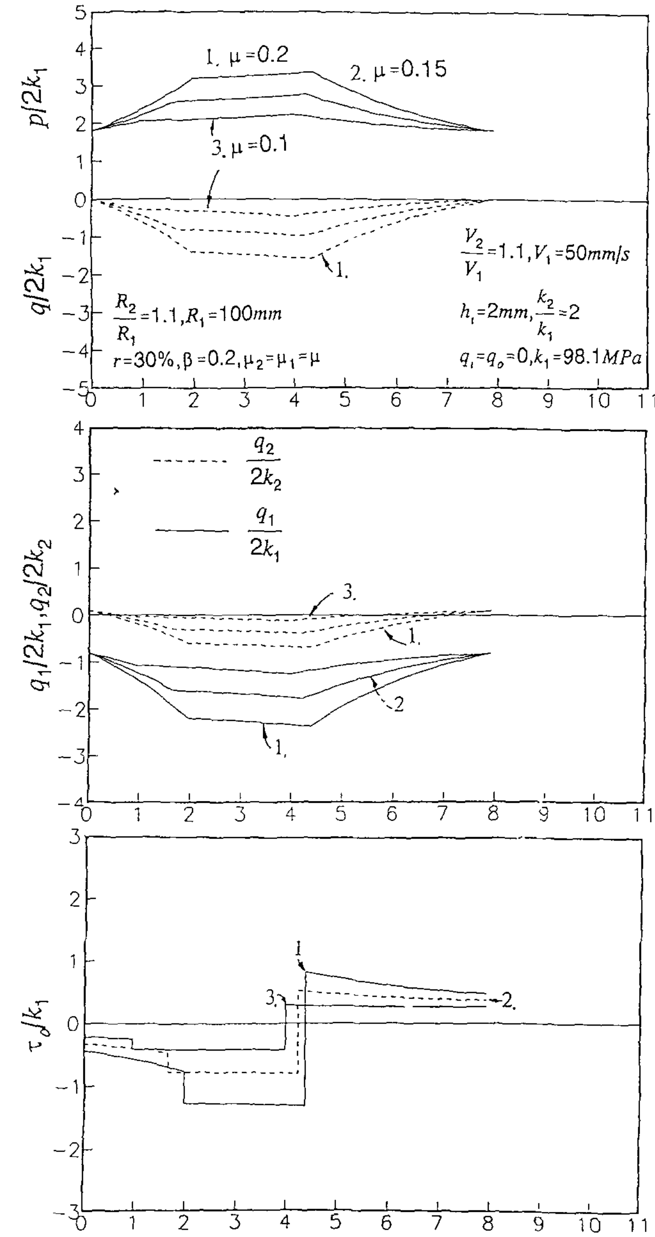

Fig. 8 Effects of frictional coefficient, μ, on various stress distributions at the roll gap

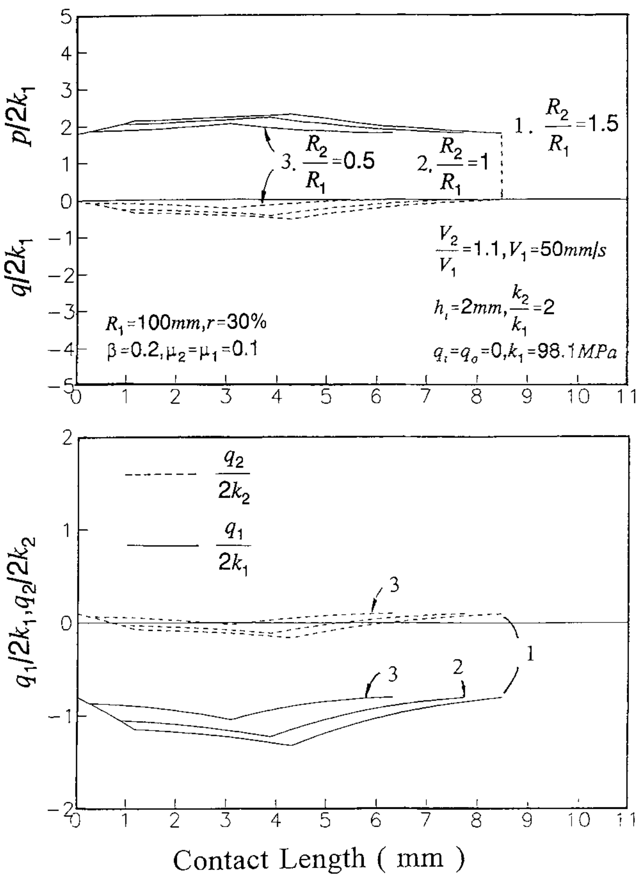

Fig. 9 Effects of roll radius ratio, R_2/R_1, on various stress distributions at the roll gap

Figure 9 shows the effects of roll radius ratio, R_2/R_1, on the various stress distributions at the roll gap. It is observed that $p/2k_1$, $q/2k_1$ and $q_1/2k_1$, decrease with decreasing R_2/R_1 (R_1 is fixed), whereas $q_2/2k_2$ changes the stress state to a tensile condition at the entrance and exit of the roll gap.

Figure 10 illustrates the effects of roll speed ratio, V_2/V_1, on the various stress distributions at the roll gap. The magnitude of $p/2k_1$, $q/2k_1$, $q_1/2k_1$, $q_2/2k_2$, and τ_o/k_1 decreases with increasing V_2/V_1, whereas $q_2/2k_2$ changes the stress state to a tensile condition at the entrance and exit of the roll gap as roll speed ratio increases.

Variations of rolling forces and rolling torques with roll radius ratio, R_2/R_1, for various thickness ratios are shown in Fig. 11(a) and (b), respectively. Rolling forces and torques are calculated by Eq 33 and 39. Evidently, both rolling force and rolling torque decrease with increasing β under a fixed roll radius ratio, and they increase with increasing R_2/R_1 under a fixed thickness ratio, β.

The analytical results for the specific rolling pressure $p/2k_1$, specific horizontal stress $q/2k_1$, specific shear stress at the interface of the clad sheet τ_o/k_1, rolling force per unit width P, and so forth, are summarized in Table 2, where the "up" and "down" arrows indicate that the analytical results either increase or decrease, respectively, with the corresponding rolling condition.

Table 2 confirms that:

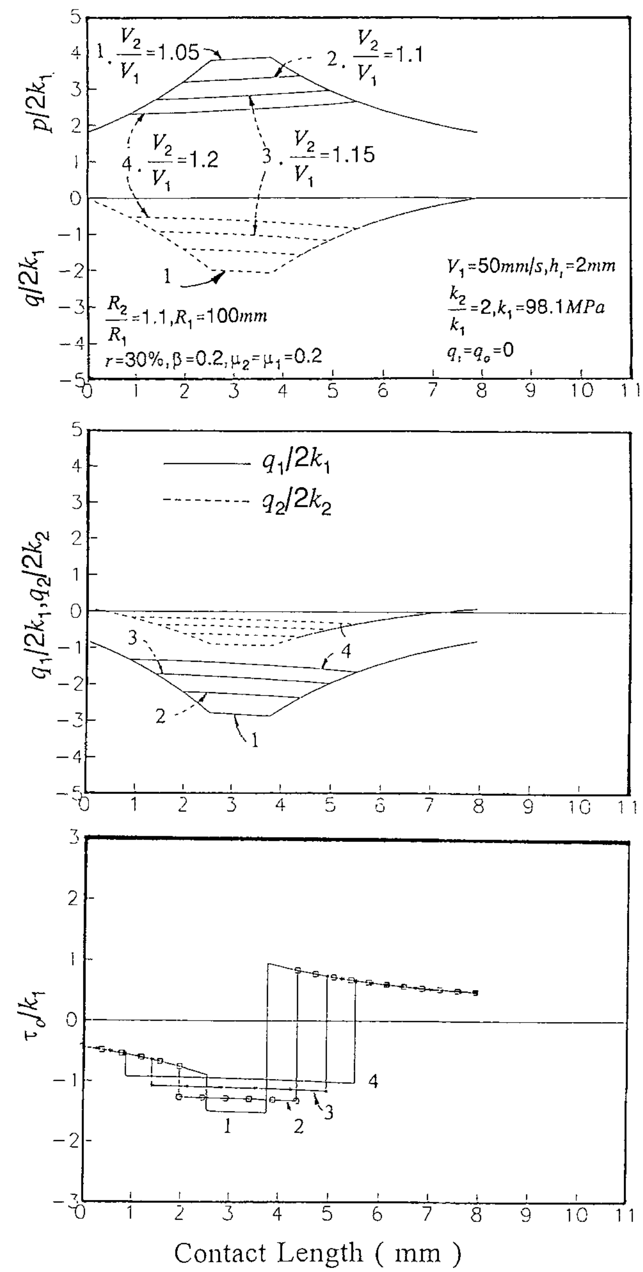

Fig. 10 Effects of roll speed ratio, V_2/V_1, on various stress distributions at the roll gap

- The magnitude of $p/2k_1$, $q/2k_1$, τ_o/k_1, P, and T decreases with increasing thickness ratio (β) and roll speed ratio (V_2/V_1).
- $p/2k_1$, $q/2k_1$, τ_o/k_1, P, and T, increase with increasing reduction (r), frictional coefficient (μ), roll radius ratio (R_2/R_1), and shear yield stress ratio (k_2/k_1).

4. Conclusions

This work proposed an efficient analytical model for a general asymmetrical cold rolling of clad sheet to explore the char-

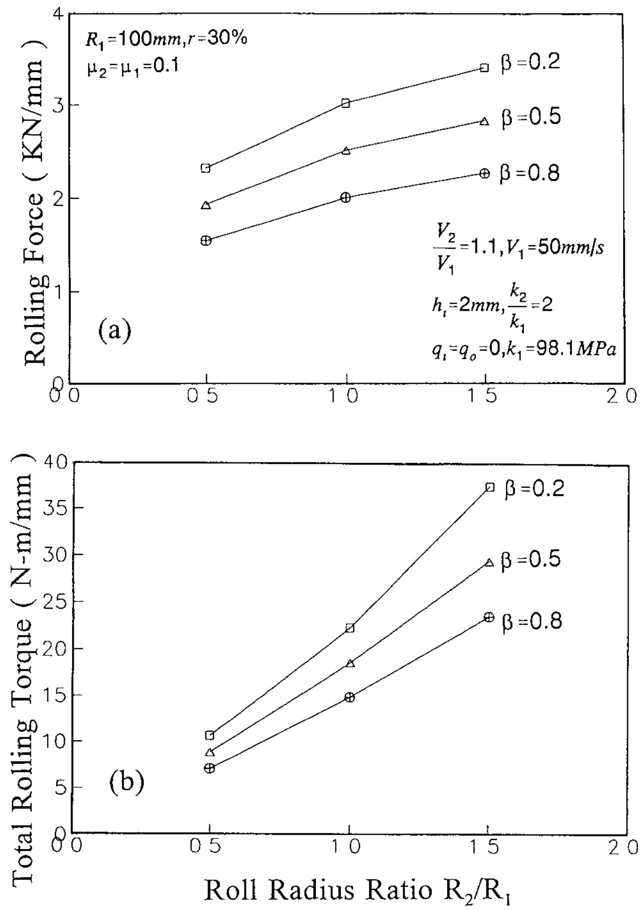

Fig. 11 Variations of rolling force and rolling torque with roll radius ratio for various thickness ratios

acteristics of clad sheet bonded before rolling. Prediction of rolling pressure and horizontal stress distributions of the whole clad sheet, horizontal stress distributions in the component layers, shear stress at the interface of the clad sheet, and rolling force under conditions of different roll radii and speeds could be achieved easily and rapidly. The computational time required by this analytical model is about 1/20 to 1/25 of that required by the RUNGE KUTTA numerical method under the same rolling conditions.

Table 2 Summary of analytical results for the asymmetrical cold rolling of clad sheet

Rolling condition	Analytical results $p/2k_1$	$q/2k_1$	τ_0/k_1	P	T
β	↓	↓	↓	↓	↓
r	↑	↑	↑	↑	↑
μ	↑	↑	↑	↑	↑
V_2/V_1	↓	↓	↓	↓	↓
R_2/R_1	↑	↑	↑	↑	↑
k_2/k_1	↑	↑	↑	↑	↑

Note: ↑, increase; ↓, decrease

References

1. M. Nakamura, S. Maki, T. Matsuda, and N. Nagai, Cold Bonding of Metal Sheets Using Mutual Sliding by Modified Contact Differential Speed Rolling, *J. Jpn. Soc. Technol. Plast.*, Vol 29 (No. 327), 1988, 404-410
2. S. Maki, M. Nakamura, T. Matsuda, and N. Nagai, Influence of Rolling Condition on Bond Strength in Cladding of Steel Sheet with Aluminum, *J. Jpn. Soc. Technol. Plast.*, Vol 30 (No. 336), 1989, p 71-76
3. D. Pan, K. Gao, and J. Yu, Cold Roll Bonding of Bimetallic Sheets and Strips, *Mater. Sci. Technol.*, Vol 5, 1989, p 934-939
4. S.H. Lee and D.N. Lee, Slab Analysis of Roll Bonding of Silver Clad Phosphor Bronze Sheets, *Mater. Sci. Technol.*, Vol 7, 1991, p 1042-1050
5. H. Dyja and M. Pietrzyk, On the Theory of the Process of Hot Rolling of Bimetal Plate and Sheet, *J. Mech. Work. Technol.*, Vol 8, 1983, p 309-325
6. A.G. Mamalis, N.M. Vaxevanidis, and D.I. Pantelis, On the Rolling of Bimetallic Explosively Cladded Plates, *Proc. 4th Int. Conf. Technology of Plasticity*, 1993, p 874-879
7. M. Kiuchi and Y.M. Hwang, Study on Complex Asymmetrical Rolling, Part I: Mathematical Model of Complex Asymmetrical Rolling, *J. Jpn. Soc. Technol. Plast.*, Vol 30 (No. 344), 1989, p 1308-1315
8. M. Kiuchi, Y.M. Hwang, and K. Shintani, Study on Complex Asymmetrical Rolling, Part II: Analysis and Experiment on Complex Asymmetrical Rolling, *J. Jpn. Soc. Technol. Plast.*, Vol 30 (No. 344), 1989, p 1316-1323
9. M. Kiuchi and Y.M. Hwang, Study on Complex Asymmetrical Rolling, Part III: Effects of Rolling Conditions on Bonding Factors in Clad Sheet Rolling, *J. Jpn. Soc. Technol. Plast.*, Vol 31 (No. 357), 1990, p 1253-1258
10. M. Kiuchi, Y.M. Hwang, and K. Shintani, Study on Complex Asymmetrical Rolling, Part IV: Analysis and Experiment on Sandwich Sheet Rolling, *J. Jpn. Soc. Technol. Plast.*, Vol 31 (No. 359), 1990, p 1445-1450
11. H. Suzuki, J.I. Araki, and K. Shintani, A Study on Rolling of Double-Layer Metal Plate, *J. Jpn. Soc. Technol. Plast.*, Vol 13 (No. 133), 1972, p 114-121
12. H. Suzuki, J.I. Araki, and M. Aiba, An Analytical Study on Mechanics in Roll Bonding of Double-Layer Metal Sheets, *J. Jpn. Soc. Technol. Plast.*, Vol 15 (No. 166), 1974, p 931-937
13. Y.M. Hwang and G.Y. Tzou, An Analytical Approach to Asymmetrical Cold Strip Rolling Using the Slab Method, *J. Mater. Eng. Perform.*, Vol 2 (No. 4), 1993, p 597-606